



Corrosion resistance of zinc-iron coated plates of high-tensile steel by stepwise rapid heating

Yilin Wang[†], Dongyu Fang, Bin Zhu, Liang Wang and Yisheng Zhang

State Key Laboratory of Materials Processing and Die & Mould Technology, Huazhong University of Science and Technology, Wuhan 430074, China

[†]E-mail: wangyilin@hust.edu.cn

The hot stamping technology of ultra-high-strength boron steel is an effective way to lighten the weight of automobiles. High-strength steel zinc-iron (GA) coated plates have the dual roles of barrier and cathodic protection, and have a broad application prospect in the field of boron steel hot stamping. How to control the heat treatment process to achieve the optimal balance of the plating organization, protective properties and matrix properties is the core issue in industrial application. The influence mechanism of different pre-oxidation time and austenitization temperature holding time on the matrix properties and plating organization characteristics under the stepped rapid heating process was investigated. Firstly, the polarization curves were obtained through electrochemical characterization tests to qualitatively evaluate the cathodic protection performance of zinc-iron plating in different states; then the macroscopic corrosion behaviors of zinc-iron plated plates in the original state, plated plates and bare plates under different heating processes were comparatively analyzed through neutral salt spray tests; finally, the range of rapid heating processes for plating in obtaining better corrosion resistance was summarized in combination with the high-temperature characteristics of plated plates under the rapid heating process.

Keywords: Hot stamping; High-strength steel; Zinc-iron plating; Rapid heating; Corrosion resistance.

1. Introduction

Automotive lightweighting is the use of new materials and process technologies to minimize the weight of the vehicle without sacrificing the safety of the vehicle, thus reducing fuel consumption and exhaust emissions. In recent years, high-strength steel hot stamping and forming parts have been widely used in automobile body structural parts, such as A/B pillars, bumpers, and laser splicing plate door rings. Boron steel austenitizing heating and deformation are at high temperatures, the surface of the steel plate will be oxidized to form oxide skin, resulting in decarburization of the surface of the part, resulting in non-uniformity of the organization and properties of the part. In the subsequent forming, the oxidized skin will increase the friction coefficient between the mold and the steel plate, aggravate the wear of the mold, and reduce the life of the mold. In order to effectively avoid the occurrence of oxidation and decarburization of steel plates, plating technology is widely used for surface protection of automotive hot stamped boron steel [1,2]. According to the elemental composition of the coating, the surface coating system of hot stamped high-strength steel includes aluminum-silicon coating, zinc-based coating, zinc-nickel coating, composite coating, etc. Among them, zinc-based coating has a broad development

prospect in the field of hot stamping of high-strength steel because of its dual role of barrier protection and cathodic protection.

During the service period of automobile, chemical or electrochemical corrosion will occur in the parts due to the environment and working conditions, and the good or bad corrosion resistance directly affects the service life of the parts, and even threatens the safety of automobile. For this reason, it is necessary to use based on electrochemical characteristics test experiments and neutral salt spray test, the zinc and iron coated plate under different rapid heating process in the service process of corrosion resistance behavior of a comprehensive assessment.

1.1. Stepped rapid heating

High-temperature tensile experiments were conducted on zinc-iron coated high-strength steel plates using a Gleeble thermal simulation testing machine in an air atmosphere. The experimental materials and specimen dimensions are depicted in Fig. 1. Table 1 and Fig. 2 illustrate the process parameters and schematic diagrams of the specimen's rapid heating and high-temperature deformation. Two sets of specimens were subjected to high-temperature tensile experiments to analyze the alloying characteristics of the coatings under different degrees of alloying and deformation temperatures. The pre-oxidation and austenitization temperatures were 820 °C and 885 °C, respectively, with a pre-oxidation duration of 40 seconds. The high-temperature stress-strain curves of both coated and uncoated specimens were compared to assess the effects of plating conditions on the substrate's high-temperature formability and to detect any signs of Liquid Metal Induced Embrittlement (LMIE) leading to premature fracture.

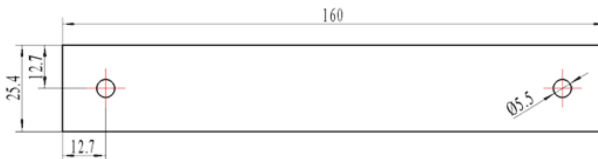


Fig. 1 Specimen for plating organization analysis

Table 1 Stepped rapid heating and deformation temperature process parameters

| Category | Austenitizing holding time (s) | Deformation temperature (°C) |
|------------------------------------|--------------------------------|------------------------------|
| Different alloying degree | 20/50/80/130 | 850 |
| Different deformation temperatures | 20 | 820/780/750/720/690/660 |
| | 50 | 820/780/750 |

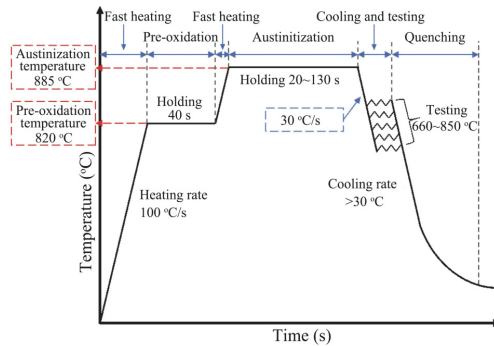


Fig. 2 Schematic diagram of stepwise rapid heating and high temperature deformation process path

2. Experimental materials and methods

2.1. Experimental materials

The experimental materials were selected from the stepped fast heating zinc-iron coated plates with different alloying degree of plating to carry out electrochemical characterization experiments and neutral salt spray corrosion experiments, meanwhile, the original zinc-iron coated plates, bare plates and zinc-iron coated plates under the traditional furnace radiant heating were used as the control group, and the specific process parameters are shown in Table 2. All heat treatment processes were carried out on a Gleeble thermal simulation tester.

Table 2 Heating process of different experimental materials and analyzed experiments

| Experimental materials | 820 °C pre-oxidation holding time (s) | 850 °C austenitization holding time (s) | Electrochemical properties test experiment | Neutral salt spray corrosion experiment | Category No. |
|---|--|---|--|---|-----------------------------|
| Stepped rapid heating | 40 | 20 | ✓ | ✓ | RH40 s + 20 s |
| | | 50 | ✓ | — | RH40 s + 50 s |
| | | 100 | ✓ | ✓ | RH40 s + 100 s |
| Radiant heating of zinc-iron coated sheets in the furnace | — | 190 | ✓ | ✓ | Radiant heating 190 s |
| | — | 300 | — | — | Radiant heating 300 s |
| Zinc-iron coated plate in its original state | — | — | — | ✓ | — |
| Bare plate | — | — | — | ✓ | — |

The heating rate and pre-oxidation process parameters of the zinc-iron coated plates for the stepwise rapid heating process were 100 °C/s and 820 °C holding time of 40 s, respectively; the alloying state of the coatings under the rapid heating process corresponded to three grades of low, medium and complete, respectively. The zinc-iron coated plates

were supplied in their original state, and the bare plate specimens were obtained by grinding away the galvanized layer. The degree of alloying of the coatings under the furnace radiation heating process is complete alloying with 190 s holding time and over-alloying with 300 s holding time.

2.2. Electrochemical characterization tests

The electrochemical testing experiments were carried out at room temperature using a ZH760 electrochemical workstation and accompanying software to obtain the polarization curves of the materials. A three-electrode system was used for the tests, with the electrolyte being a 5.0 wt% NaCl solution, the reference electrode being a saturated calomel electrode, the test sample being the working electrode, and the auxiliary electrode being a Pt electrode.

Figure 3 shows the specimen preparation process for the electrochemical characterization test experiment. First, a precision cutter was used to cut the heated zinc-iron plated plate, retaining a homogeneous temperature zone with a width of 10 mm. Then, the plated surface was ultrasonically cleaned for 15 min to remove most of the oxides. Finally, the test side of the specimen was placed in close contact with the bottom of the mold and sealed by pouring high-temperature liquid paraffin to ensure that only the test side was exposed and the other five sides were sealed. This was designed to ensure that only one side of the plating was in contact with the electrolyte in order to test and compare the electrochemical properties of the plating. A test area of 1 cm² was used in the experiments with a scan rate of 1 mV/s.

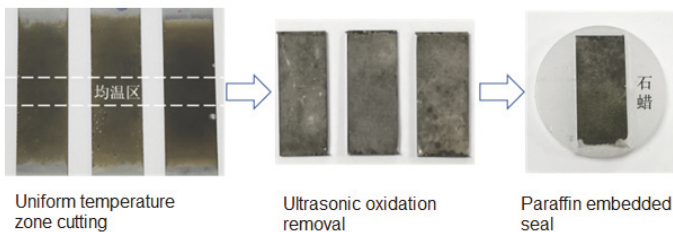


Fig. 3 Preparation steps of experimental specimens for electrochemical characterization test

2.3. Neutral salt spray corrosion test

Neutral salt spray corrosion test refers to the Chinese standard GE/T 10125-2012 (artificial atmosphere corrosion test - salt spray test) in the NSS test, the experimental instrument selection of precision salt spray tester. Salt solution used in the experiment is 5.0 wt.% of NaCl solution, jet tower nozzle under pressure, continuous salt spray to the salt spray chamber, salt spray deposition amount of 1.5 "±" 0.5 mL/80 cm²-h, collected solution PH value to ensure that 6.5 ~ 7.2 between the temperature of the test chamber for 35 "±" 2 °C, humidity greater than 95%.

The preparation method of the specimen used in the salt spray corrosion experiment is shown in Figure 4. First of all, the heat-treated zinc-iron plating plate is cut down using a cutting machine in the homogeneous temperature zone, and then use ultrasonic cleaning

machine to remove surface oxides and impurities, and then use anhydrous ethanol to clean the surface of the specimen and blow-drying, and finally use the waterproof tape to seal the specimen on the side and the back, to ensure that only one side of the plating layer is exposed out of corrosion occurs, and the area of the exposed area is roughly $22 \text{ mm} \times 10 \text{ mm}$. In addition, the bare boards and the original state of zinc-iron plating In addition, bare plates and in-situ zinc-iron plated plates only need to be cleaned and sealed. When the prepared specimens are placed in the specimen racks, the test surface should be 15° to 30° to the vertical, and the specimens should be spaced apart to avoid the salt spray collecting on the surface of the specimens or falling onto other specimens.

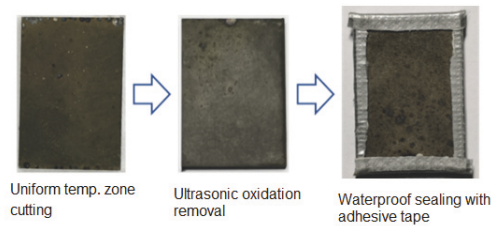


Figure 4 Neutral salt spray test specimen preparation

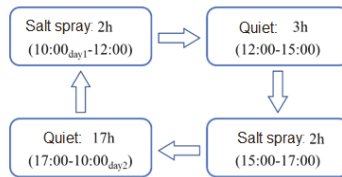


Fig. 5 Flow chart of neutral salt spray test on galvanized iron coated plate of high tensile steel

According to the requirements of Chinese standards and laboratory safety regulations, the experiment is set up for a total of six cycles, each cycle length of 24 h, the process shown in Figure 5. Specimens first corrode in a salt spray atmosphere after 2h, after the end of ten minutes after the removal of fog and stand for 3h; then continue to corrode in a salt spray atmosphere for 2h, after the removal of fog in the static to the beginning of the next cycle. A total of three groups of specimens were prepared, and one group of specimens was taken out at the end of the even-numbered cycles during the experimental process, and the surface and cross-section corrosion morphology was observed using an optical microscope.

3. Experimental results and analysis

3.1. Experimental analysis of electrochemical properties

Figure 6a shows the Tafel polarization curves, self-corrosion potentials and self-corrosion current densities under different heating processes. The self-corrosion potential, which is the potential when the metal reaches a stable corrosion state, shows the potential difference between the zinc-iron plating layer and the substrate. The larger the potential difference, the stronger the cathodic protection. Self-corrosion current is the electrode current under

the corrosion potential, reflecting the corrosion rate under the condition of no applied current. The size of the self-corrosion current density of the zinc-iron coating affects the corrosion rate, the greater the rate, the shorter the effective cathodic protection time.

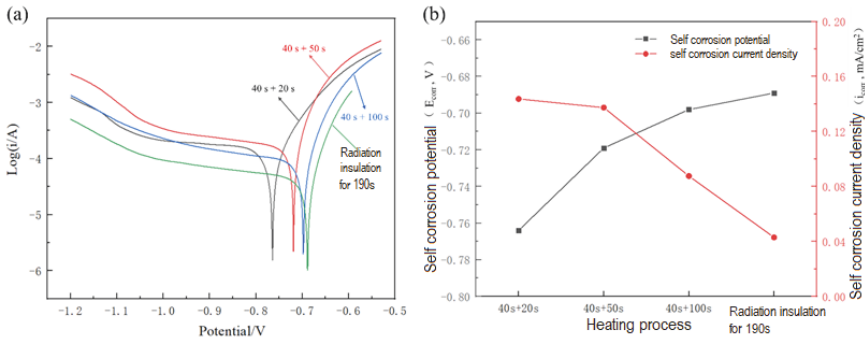


Fig. 6 Polarization curves and self-corrosion potentials and current densities of zinc-iron coated plates under different heating processes

From Fig. 6b, it can be observed that in the stepped rapid heating process, the different holding time of austenitization temperature affects the alloying degree and cathodic protection ability of the plating. When the holding time is 20 seconds, the plating has the lowest alloying degree, the smallest Fe element content and self-corrosion potential (-0.764 V), and exhibits the strongest cathodic protection ability. As the holding time was increased to 50 seconds, the alloying degree of the coating increased, the Zn element content decreased, the self-corrosion potential increased to -0.719 V, and the cathodic protection ability decreased. After the holding time was extended to 100 seconds, the plating layer was completely alloyed, the Zn content was the lowest, the self-corrosion potential increased to -0.698V, and the cathodic protection ability was further weakened. The plated layer after 190 seconds of radiant heating in the furnace, with lower Zn elemental content and a self-corrosion potential of -0.689 V, showed the weakest cathodic protection. In addition, with the increase of austenitization holding time, the Zn element content decreased slowly and the rate of increase of self-corrosion potential slowed down. The self-corrosion current density of the plating decreases with the austenitization holding time, indicating that the alloying degree of the plating increases and the corrosion rate slows down. Specifically, the plated layer after 190 seconds of radiant heating in the furnace had the lowest self-corrosion current density of 0.04 mA/cm², showing the lowest corrosion rate.

In the stepped rapid heating process, as the austenitization temperature holding time increases, the alloying degree of the plating layer increases, the self-corrosion potential increases, the self-corrosion current density decreases, the cathodic protection weakens, and the overall corrosion rate decreases. The cathodic protection of fully alloyed plating under the furnace radiation heating process is weaker than that of fully alloyed plating under the rapid heating process, but the corrosion rate is smaller. In addition to the electrochemical properties, the phase structure, organization, thickness and elemental distribution of the plated layer also affect the corrosion behavior and overall corrosion

resistance. Further studies should be combined with neutral salt spray corrosion experiments to investigate the macroscopic corrosion behavior of the coatings.

3.2. Neutral salt spray corrosion experimental analysis

The cross-sectional morphology and surface XRD diffraction patterns of the six specimens before the experiment are shown in Figures 7 and 8. The as-constructed galvanized plate layer is mainly composed of δ phase, and the diffraction peaks of the thin Γ layer located at the lower layer/substrate interface are not visible in the XRD patterns, and the interface between the layer and the substrate is clear; the layer under the condition of RH40 s + 20 s consists of α -Fe(Zn) phase and a small amount of Γ phase, and the Γ phase is mainly distributed in the surface area of the layer; the layer under the conditions of RH40 s + 100 s, radiant heating of 190 s and radiant heating of 300 s has all completed alloying; the layer under the condition of RH40 s + 100 s, radiant heating of 300 s has all completed alloying. RH40 s + 100 s, radiation heating for 190 s and radiation heating for 300 s. The plated layer under the condition of RH40 s + 100 s is completely alloyed and consists of only α -Fe(Zn) phase, and the interface between the plated layer and the substrate becomes blurred. In addition, after ultrasonic cleaning, most of the oxide layer on the surface of the heat-treated ZnFe plated plate was removed, and the intensity of the corresponding ZnO diffraction peaks decreased significantly.

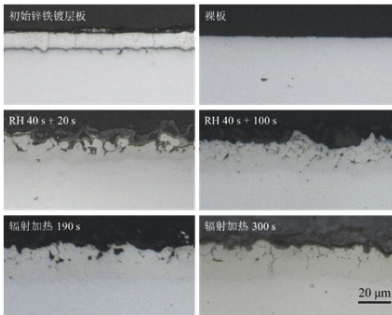


Fig. 7 Cross-sectional organization and morphology of different specimens before corrosion

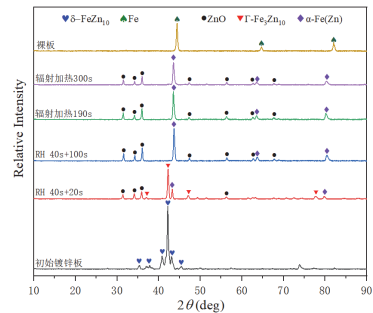


Fig. 8 XRD diffraction patterns of different specimens before corrosion

Figure 9 shows the surface corrosion states of the six test specimens under 2, 4 and 6 cycles of neutral salt spray, respectively, and the specimens are, from left to right, as-is zinc-iron coated plate, RH40 s + 20 s, RH40 s + 20 s, radiant heating for 190 s, radiant heating for 300 s, and bare plate. Comparison shows that, under the same corrosion cycle, the surface color gradually becomes darker from left to right; the surface of the as-received zinc-iron coating is the lightest gray-white color; the bare plate is reddish-brown and locally black; the surface color of the zinc-iron coating under the rapid heating process is gray-white and reddish-brown; the gray-white area on the surface of the zinc-iron coating under the radiant heating process is reduced significantly compared to that under the rapid heating process, and the surface color is basically all gray-white at the time of holding heat for 300 s. The surface color of zinc-iron coating is reddish brown. According to the

literature [5], the gray-white area is white rust, which is mainly composed of zinc compounds; the reddish-brown area is red rust, which is mainly composed of iron oxides, and both of them show a loose structure under the microscope.

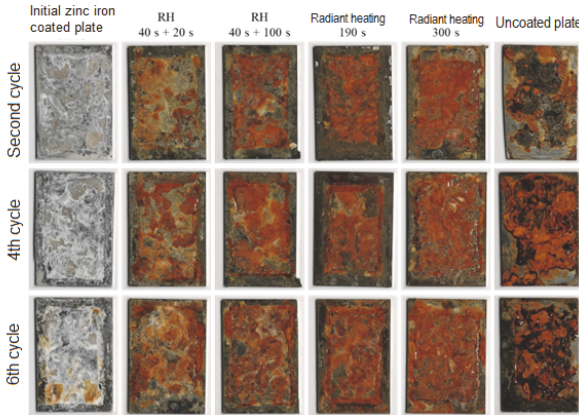


Fig. 9 Surface morphology of different experimental specimens under different corrosion cycles

With an increase in the number of corrosion cycles, the bare plate specimens gradually exhibited a deepening color and the appearance of a noticeable rust layer. Initially, in the zinc-iron coated plate, the white rust was not continuous and showed no significant changes in the second cycle. However, in the fourth cycle, the white rust increased in quantity and thickness. By the sixth cycle, the white rust covered the entire surface, accompanied by the emergence of a light red rust. In the RH40s + 20s process, the white rust appeared deeper and the red rust was less pronounced. As time progressed, the white rust decreased, resulting in a deepening color, while the red rust increased. In the RH40s + 100s process, the white rust decreased and the red rust increased. During the radiant heating process, when held for 190s, the white rust decreased and the red rust increased. When held for 300s, the white rust was predominantly converted to red rust, with little white rust remaining.

Through the observation of cross-section microstructure and morphology, the zinc and iron coated plate under different processes is compared with the bare plate under different corrosion cycles, as shown in Figure 10. Bare plate with the extension of the corrosion cycle, the depth of corrosion pits and product thickness gradually increased, the 6th cycle corrosion pit depth of up to 35.55 μm . the original state of zinc and iron coated plate in the 2nd cycle corrosion mainly occurs in the upper part of the plating layer, the depth of 7.11 μm or less; to the 4th cycle of the corrosion area increased significantly, but did not extend to the substrate; the 6th cycle of the corrosion accelerated, the plating layer corrosion is complete, and the substrate appeared in the corrosion of the pits, up to the depth of 19.72 μm . The heat-treated zinc-iron plating corrosion is slower and mainly occurs in the plating layer with better corrosion resistance. In RH40s + 20s process, to the 2nd cycle of the plating layer has obvious corrosion, mainly in the upper layer, at the same time, there is a black spot in the middle and upper part of the plating layer; with the growth of time, the corrosion layer from the upper gradually downward expansion, the average thickness of

the average thickness from the uniform gradual change to the thickness of the thickness of the thin and the uncorroded area gradually become thin.

Under the RH40s+20s process, the phenomena of different corrosion cycles observed by XRD diffraction patterns are shown in Fig. 11. The initial coating contained high Γ phase content, while the Γ phase completely disappeared after 2 cycles of corrosion; the intensity of the α -Fe(Zn) phase peaks gradually decreased; and the corrosion products were alkaline $Zn_5(OH)_8Cl_2 \cdot H_2O$ and hydroxyl iron oxide β -FeOOH, which appeared as white and light reddish-brown, respectively. The results show that under the RH40s+20s process, the alloying degree of the plating is low, and the Γ phase with high Zn content is corroded first, and the Γ phase around the massive α -Fe(Zn) in the middle-upper region of the plating is transformed into a black speckled distribution after corrosion.

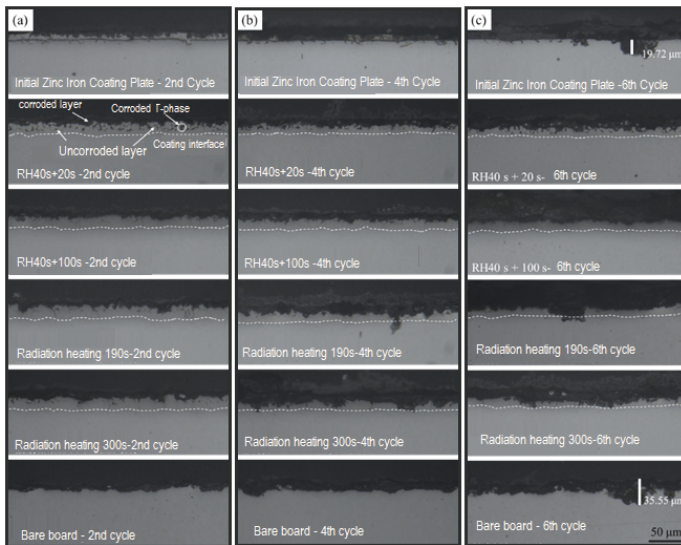


Fig. 10 Changes in cross-section corrosion morphology of different experimental specimens under different corrosion cycles:(a) 2nd corrosion cycle; (b) 4th corrosion cycle; (c) 6th corrosion cycle

Under the RH40s+100s process, the plated layer consists of α -Fe(Zn) phase without black spots; the uncorroded area of the plated layer gradually becomes thinner, and the corroded layer thickens but is more uniform. Compared with rapid heating, radiation heating corrosion is more serious, the 2nd cycle is more similar but localized corrosion pits appeared; the 4th cycle corrosion aggravated, corrosion deeper, the 6th cycle further aggravated, holding time 300s plating corrosion to the substrate. After the holding time is extended, the corrosion of the plating layer is more serious, and the uncorroded area becomes thin. The plating layer performs better under RH40s + 100s process.

Figure 12 shows the ratio of the thickness of the uncorroded area of the plated layer to the thickness of the original plated layer, i.e. the "percentage", at different etching cycles. As the corrosion cycle grows, the percentage under different heating processes gradually decreases, reflecting the trend of corrosion layer thickening and corrosion resistance

weakening. In the first 2 cycles, radiant heating 190 s and RH40 s + 20 s processes showed better corrosion resistance, accounting for more than 68%; in contrast, radiant heating 190 s had the worst corrosion resistance. By cycle 4, the share of RH40 s + 20 s and radiant heating processes decreased dramatically, and the corrosion resistance was significantly weakened, with decreases ranging from 16% to 27%. At this stage, the worst corrosion resistance was obtained for the radiant heating 300 s, whereas the percentage of RH40 s + 100 s decreased by only 7%, with better corrosion resistance. Extended to cycle 6, the corrosion resistance of RH40 s + 100 s remained the best, while the over-allayed plating at 300 s of holding exhibited the worst corrosion resistance.

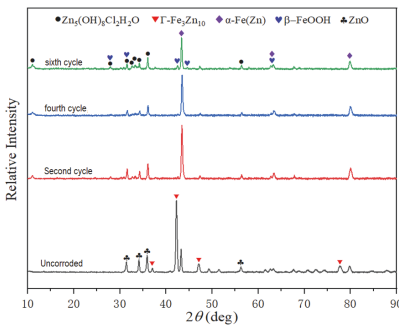


Fig. 11 XRD diffraction patterns of plated layers with different corrosion cycles under RH40 s + 20 s process.

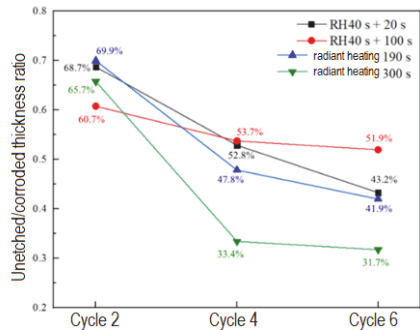


Fig. 12 Variation of the average percentage of uncorroded areas of the plating at different corrosion cycles

In addition, the ratio of the average thickness of the uncorroded area of the plated layer after corrosion to the average thickness of the plated layer before the corrosion experiment can be used as an index to measure the corrosion resistance of the plated layer, as shown in Figure 13. The smaller the ratio of the average thickness of the uncorroded area of the plated layer to the average thickness of the plated layer under the same corrosion cycle, the larger the ratio of the thickness of the corroded layer of the plated layer, the faster the corrosion rate and the worse the corrosion resistance.

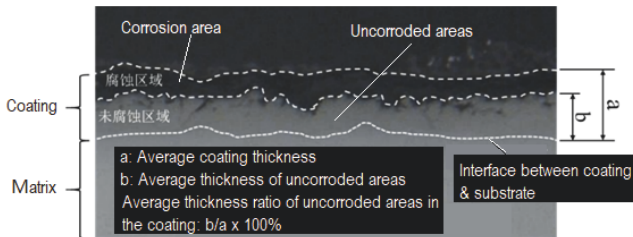


Fig. 13 Calculation of the average plating percentage in the uncorroded area of the plated layer

In the corrosion time of 2 cycles, the plating layer with RH40 s + 100 s process showed the fastest corrosion rate and the worst corrosion resistance. From the 2nd cycle to the 4th cycle, the average thickness of the uncorroded area of the plated layer under the RH40 s + 20 s process and the radiant heating process decreased rapidly, the corrosion rate of the plated layer was accelerated greatly, the thickness of the corroded layer increased rapidly,

and the corrosion resistance deteriorated rapidly. The RH40 s + 100 s process resulted in the slowest corrosion rate and better corrosion resistance, with the average thickness of the uncorroded area decreasing by only 7%. When the corrosion time is extended from the 4th cycle to the 6th cycle, the average thickness of the uncorroded area under all processes decreases by only 1.7% to 9.6%, which is obviously smaller than that of the first two cycles, and the corrosion rate of the plated layer is slowed down, which indicates that when the corroded layer reaches a certain thickness, it will inhibit the further corrosion of the plated layer. Among them, the average thickness of the uncorroded area of the plated layer under the RH40 s + 100 s process is still the smallest, the corrosion resistance is the best and the most stable, and it can provide a long-time cathodic protection performance for the substrate. In conclusion, the corrosion resistance of the plated layer under the step rapid heating process is better than that of the plated layer under the radiant heating process, the corrosion resistance of the fully alloyed plated layer is better than that of the incompletely alloyed plated layer, and the corrosion resistance of the over-alloyed plated layer will deteriorate.

4. Conclusion

The electrochemical characteristics and corrosion behavior of zinc-iron coated sheets of high-strength steel in service under different stepwise rapid heating processes were investigated by electrochemical characterization tests and neutral salt spray tests. The corrosion resistance of galvanized steel sheets in different states was comprehensively evaluated from various aspects by comparing the galvanized sheets in their original state, bare sheets and radiantly heated zinc-iron coated sheets. The main conclusions are as follows:

(1) The electrochemical characterization test shows that under the stepped rapid heating process, the alloying degree of the zinc-iron plating layer gradually increases with the increase of the holding time of the austenitization temperature, the self-corrosion potential of the plating layer gradually increases, and the self-corrosion current density gradually decreases, which indicates that the cathodic protection ability of the plating layer gradually decreases and the corrosion rate gradually decreases. Initial completion of fully alloyed plating, cathodic protection under the radiant heating process is weaker than the step-type rapid heating process.

(2) Neutral salt spray test showed that the bare plate appeared obvious corrosion pits, up to 35.55 μm , zinc and iron plating can effectively protect the substrate from corrosion. After heat treatment of zinc-iron plating, the Γ phase with higher Zn content is corroded preferentially, and after 6 cycles of corrosion, there still exists a certain thickness of uncorroded area of the plating, the substrate is not corroded, and the surface of the plating shows the morphology of white rust and red rust distributed intermittently. After 6 cycles of corrosion of the as-received zinc-iron coated plate, all the plating layer was corroded, and corrosion pits appeared on the substrate, with a depth of up to 19.72 μm , and the corrosion resistance was poor. The corrosion resistance of the plating layer under the stepped rapid heating process is better than that under the radiant heating, and the corrosion

resistance of the plating layer with preliminary complete alloying is also better than that of the plating layer with incomplete alloying, and the corrosion resistance of the plating layer with over-alloying becomes worse. When corrosion is carried out to a certain extent, the corrosion layer will inhibit further corrosion of the plating layer.

(3) make the plating corrosion resistance is the best and most stable, can provide long time cathodic protection for the substrate step fast heating process for: zinc and iron plating plate to 100 °C/s heating rate heating to 820 °C pre-oxidation 40 s, and then the same heating rate heating to 885 °C heat preservation for 100 s; at this time, the plating state for the initial alloying is completed, the average thickness of the plating of the region of the average thickness of the corrosion-free in the average thickness of the uncorroded area of the coating decreases the least in the last 4 corrosion cycles, and it is the largest after 6 corrosion cycles, which is 52%.

References

1. H. Järvinen, M. Honkanen, M. Patnamsetty, S. Järn, E. Heinonen, H. Jiang, et al. Press hardening of zinc-coated boron steels: Role of steel composition in the development of phase structures within coating and interface regions. *Surface and Coatings Technology*, 2018, 352: 378-391
2. Z. X. Gui, K. Wang, Y. S. Zhang, B. Zhu. Cracking and interfacial debonding of the Al-Si coating in hot stamping of pre-coated boron steel. *Applied Surface Science*, 2014, 316: 595-603
3. Yilin Wang, Dongyu Fang, Liang Wang, and Yisheng Zhang. Rapid Heating Process of High Strength Steel Zinc-Iron Coated Plate and Its Effect on Deformation Characteristic. K. Mocellin et al. (Eds.): *ICTP 2023, LNME*, pp. 728-735, 2024. 4.
4. Hou, Xinghui. Characterization of fluid flow in metallic pipelines and in-situ synthesis of composite ceramic coatings [Ph.D. dissertation]. Shenyang: Northeastern University, 201
5. Chen Minjuan, Chen Hao, Lu Song. Corrosion morphology of zinc and zinc alloy coatings in salt spray test. *Environmental Technology*, 2020, 38(03): 56-60.
6. Li Yadong. Influence of substrate surface condition on the organization and properties of alloyed hot-dip galvanized sheet [Master's thesis]. Kunming: Kunming University of Science and Technology, 2010

Open Access This chapter is licensed under the terms of the Creative Commons Attribution-NonCommercial 4.0 International License (<http://creativecommons.org/licenses/by-nc/4.0/>), which permits any noncommercial use, sharing, adaptation, distribution and reproduction in any medium or format, as long as you give appropriate credit to the original author(s) and the source, provide a link to the Creative Commons license and indicate if changes were made.

The images or other third party material in this chapter are included in the chapter's Creative Commons license, unless indicated otherwise in a credit line to the material. If material is not included in the chapter's Creative Commons license and your intended use is not permitted by statutory regulation or exceeds the permitted use, you will need to obtain permission directly from the copyright holder.

